THE JOURNAL OF PHYSICAL CHEMISTRY C

Article

Removal of Confined Ionic Liquid from a Metal Organic Framework by Extraction with Molecular Solvents

Manish Pratap Singh, Nilesh Ramchandra Dhumal, Hyung J Kim, Johannes Kiefer, and James A. Anderson

J. Phys. Chem. C, **Just Accepted Manuscript** • Publication Date (Web): 25 Apr 2017

Just Accepted

Removal Of Confined Ionic Liquid From A Metal Organic Framework By Extraction With Molecular Solvents.

Manish P. Singh,[1] Nilesh R. Dhumal,[2]Hyung J. Kim,[2,3] Johannes Kiefer,[1,4] James A. Anderson,[1*]

[1]Chemical and Materials Engineering Group, School of Engineering, University of Aberdeen, Aberdeen, UK, AB24 3UE.

[2]Department of Chemistry, Carnegie Mellon University, Pittsburgh, PA 15213, USA.

[3]School of Computational Sciences, Korea Institute for Advanced Study, Seoul 02455, Korea.

[4]Technische Thermodynamik and MAPEX Center for Materials and Processes, Universität Bremen, Bremen 28359, Germany.

Abstract

Hybrid materials of ionic liquids (IL) confined in metal organic frameworks (MOF) are promising materials for energy storage. The effects of exposing or treating such composite materials with molecular solvents, e.g. with the aim to extract and replace the IL, have not been studied to date. In this study, acetone, isopropanol, methanol, and water were used to remove the IL 1-ethyl-3-methylimidazolium ethyl sulfate confined in a Cu-based metal organic framework (CuBTC). The consequences of the solvent extraction process were analyzed using vibrational spectroscopy (FTIR), powder X-ray diffraction (PXRD), N_2 adsorption, scanning electron microscopy (SEM), and transmission electron microscopy (TEM). Methanol was identified as the best solvent for IL removal as it shows high extraction efficiency without affecting the porous geometry and crystal structure of the MOF. On the other hand, acetone and isopropanol were not able to completely remove the IL from CuBTC under the conditions employed. Water effectively removed the IL, but it has a significant detrimental effect on the CuBTC structure. This impact manifests as changes in the infrared spectra and the PXRD patterns as well as in the electron micrographs. The degraded CuBTC exhibits a non-porous structure that presents itself as non-uniformly agglomerated micro-rods along with very few hexagonal/amorphous phases. The confinement of acetone, isopropanol, and methanol in the MOF was also investigated. The results show that CuBTC is stable in acetone, isopropanol, and methanol but unstable in water.

INTRODUCTION

Ionic liquids (ILs) have attracted significant attention because of their potential applications in areas as diverse as carbon capture, diesel fuel desulfurization and biomass processing.[1–3] ILs have a melting point below 100°C and are composed of cations and anions.[4] The unique

properties such as low vapor pressure, flame retardancy, good thermal and chemical stability, and a wide liquid range make ILs an attractive alternative to conventional volatile organic compounds (VOCs). Moreover, ILs exhibit high ionic conductivity and wide electrochemical windows and consequently are promising electrolytes for a wide variety of electrochemical devices, such as rechargeable batteries, supercapacitors, dye-sensitized solar cells, and thermoelectric cells.[5]

Metal organic frameworks[6–14] (MOFs) are a rather new member of the family of porous materials. MOF materials combine metal-based nodes with organic linkers to build hybrid porous crystalline networks with high surface area and large pore volume. The pore size, geometry, crystal structure,shape, and functionality of the pore space can be tailored by selecting and combining suitable metal ions (Cu^{2+}, Ni^{2+}, Al^{3+}, Cr^{3+}etc.) and organic linkers (tri-carboxylate, di-pyridyl, tri-isophthalate, etc.).These tunable properties make MOFs promising materials for gas storage,[8] separations,[15] catalysis,[16] carbon capture and storage (CCS),[17] biomedicine,[18] and chemical sensors.[19]

Confining ILs in MOFs brings these fascinating classes of material together. However, the resulting hybrid materials represent an almost unexplored area. To date, most investigations havefocused on ILs in inorganic porous matrices[20] such as SiO_2,[21] TiO_2,[20] and SnO_2[22] as well as organic porous matrices such as carbon nanotubes,[23] graphene,[24] and porous carbon.[25]The hybrid material is known as an ionogel,[20] in which the IL is kept inside the porous skeleton. The IL is found to preserve its liquid like dynamics[26] in ionogels and therefore it has a high ionic conductivity. This aspect has attracted much attention due to possible applications of ionogels in electrochemical devices. In other applications, the IL was used as a templating agent to modify the pore parameters and geometry of the porous material. In this case, the IL is removed again

from the ionogel. Singh et al. [27–30] have synthesized a variety of micro to mesoporous materials *via* impregnation and subsequent removal of ILs from porous materials. In order to extract the IL, solvents such as water, acetone, and dichloromethane were used. Acetonitrile and acetone/ethanol mixtures were also used for this purpose.[31–33] Interestingly, various types of porous matrices such as silica and titanium were found to be stable in the presence of these solvents and hence these solvents along with a complex (functionalization agent) were used for functionalization of porous matrices like silica.

However, no studies have been performed regarding the impact of the solvents on MOFs with IL during post synthetic modification. This is very important as understanding how the IL and the solvents influence the chemical and structural properties of the MOF can be the key for any potential implementation of targeted chemical modifications. Otherwise, a possibility exists of interactions between the MOF and the solvent, which could modify the properties of the host-guest system. Furthermore, a better understanding of solvents with MOFs would offer a potential route for reusing the MOF after the removal of confined materials. Furthermore, a basic knowledge of materials containing conventional solvents, ILs, and MOFs would be beneficial for tailoring new composite materials, in which the IL is encapsulated in the pores of a MOF with the aid of a solvent.

One of the most extensively studied MOFs is $Cu_3(BTC)_2$. It is commonly known as Basolite^{TM} C300, HKUST-1, CuBTC, or MOF-199. CuBTC has a face centered cubic crystalline porous framework structure. It consists of three different sizes of pores. The first type of pore has a diameter of ~ 9-13.5 Å[34,35] with an accessible open copper site. These pores are centered on face and corners of the unit cell. The second type of pores has a diameter of ~ 9-11 Å[34–36] with inaccessible Cu sites and centered at the unit cell center and midpoint of the unit cell edges.

These two larger pores are arranged in an alternating manner and connected by 9 Å windows. The third and last type of pores have a diameter of ~ 5-7 Å.[34–37]

The present paper reports a systematic study of confined molecular solvents in a MOF. The solvents of interest are acetone, isopropanol, methanol, and the IL 1-ethyl-3-methylimidazolium ethyl sulfate (EMIM-ETS). The three volatile organic solvents were selected because they are very common and, despite being rather small, they contain different functional groups and have systematically varied chemical structures. The IL was chosen as it has been characterized as a neat substance[38–40] as well as in combination with CuBTC[41] and molecular solvents.[42] In the second part of the study, the effects of extracting the IL from the MOF using the above organic solvents and water are investigated. In order to gain scientific insights and a comprehensive picture including molecular, crystallographic and macroscopic effects, infrared spectroscopy, powder x-ray diffraction, N_2 adsorption, scanning electron microscopy (SEM), and transmission electron microscopy (TEM) were employed.

EXPERIMENTAL

Chemicals

Basolite^{TM} C300 and methanol (purity ≥ 99.9%) were purchased from Sigma-Aldrich. Extra dry acetone (purity 99.8%) and isopropanol (purity 99.8%) were purchased from AcroSeal^{R}. Halide-free 1-Ethyl-3-methylimidazolium ethyl sulfate was purchased from Alfa Aesar (purity 99%). Water content by Karl Fischer titration is less than 1500 ppm. The MOF and the IL are water sensitive and hence, care was taken during handling of the materials to minimize contact with the atmospheric humidity.

Confinement of IL and solvents in CuBTC

IL impregnated CuBTC samples were prepared by mixing CuBTC with the IL at a molar fraction of X_{MOF} = 20 mole%. This relationship provides a ratio of available pore volume of CuBTC and volume occupied by IL molecules of approximately two. Subsequently, the sample was heated at 60 °C for 24 h to obtain a homogeneous distribution of IL within the pores of the CuBTC. Solvent confined CuBTC samples were prepared by mixing a small amount of CuBTC with a droplet of solvent.

Washing of bulk and IL confined CuBTC with solvents and water

The pristine (as received) CuBTC samples were emerged in 10 ml of acetone, isopropanol, methanol, and water for 5 h. Then they were filtered and dried at 70 and 150 °C for 24 h at each temperature. A similar procedure was used for the removal of the IL from the IL impregnated CuBTC samples using the solvents. The IL impregnated CuBTC samples were washed twice with water to insure the removal of IL from the pores and the surface of CuBTC. Subsequently, the samples were filtered and dried at 70 ºC for 24 h.

Characterization

Vibrational spectroscopy. FTIR spectra were recorded in the range 4000 to 400 cm^{-1} using a Bruker Vertex 70 and on a Perkin-Elmer Spectrum 2 instrument with the nominal resolution of 0.5 and 4 cm^{-1}, respectively on an attenuated total reflection (ATR) module. The Bruker instrument was equipped with a diamond ATR unit (1 reflection at 45°). To obtain a suitable signal to noise ratio, 16 scans were averaged. All spectra were background corrected.

Electron microscopy. Scanning electron micrographs of the samples were obtained using a Hitachi S-520 scanning electron microscope (SEM) operated at 20kV. Transmission electron micrographs of the samples were obtained using a JEOL JEM-2000EX transmission electron

microscope (TEM) operated at 200 kV. The images were captured with a Gatan Erlangshen ES500W camera.

Adsorption isotherms. N_2 adsorption isotherms of the CuBTC samples were measured on a Micromeritics TriStar 3000 V4.02 analyzer at -196 °C. All samples were pretreated by degassing at 70 or 150 °C under dry nitrogen gas for 24 h. The specific surface area was determined from a Brunauer–Emmett–Teller (BET) plot. The total pore volume was determined using the t-plot method. The accuracy and reproducibility of the instrument was ±5 %.

X-ray diffraction. Structural changes were monitored by X-ray powder diffraction using a Panalytical X'Pert Pro diffractometer fitted with a PIXcel1D detector using Cu-Kα radiation (1.54 Å) operated at 45 kV and 40 mA and using a silicon zero-background sample holder. The measurements were performed with powders in an air-conditioned room (20 ºC, no control of humidity) in continuous scanning mode from 5-50° 2θ with a step size 0.013º and ≈2 min acquisition time.

RESULTS AND DISCUSSION

Confinement of IL

Fig. 1A shows the FTIR spectra of the pure IL (a), the pure CuBTC (c), and the IL/MOF system (b). The spectra reveal evidence for strong molecular interactions between the IL and the MOF, which manifest as changes in frequencies of vibrational modes of the IL and the MOF. A detailed spectroscopic and computational analysis of EMIM-ETS confined in CuBTC has been reported recently.[41] Data confirm a perturbation of the symmetry of the MOF structure due to the interactions between the IL anion with the Cu ions. Moreover, inside the MOF, two different types of IL ion pairs are formed: One ion-pair structure exhibits enhanced interionic interactions by strengthening the hydrogen bonding between the cation and anion, whereas the other structure

corresponds to weaker interactions between the IL cation and anion. For further details, see previous work.[41]

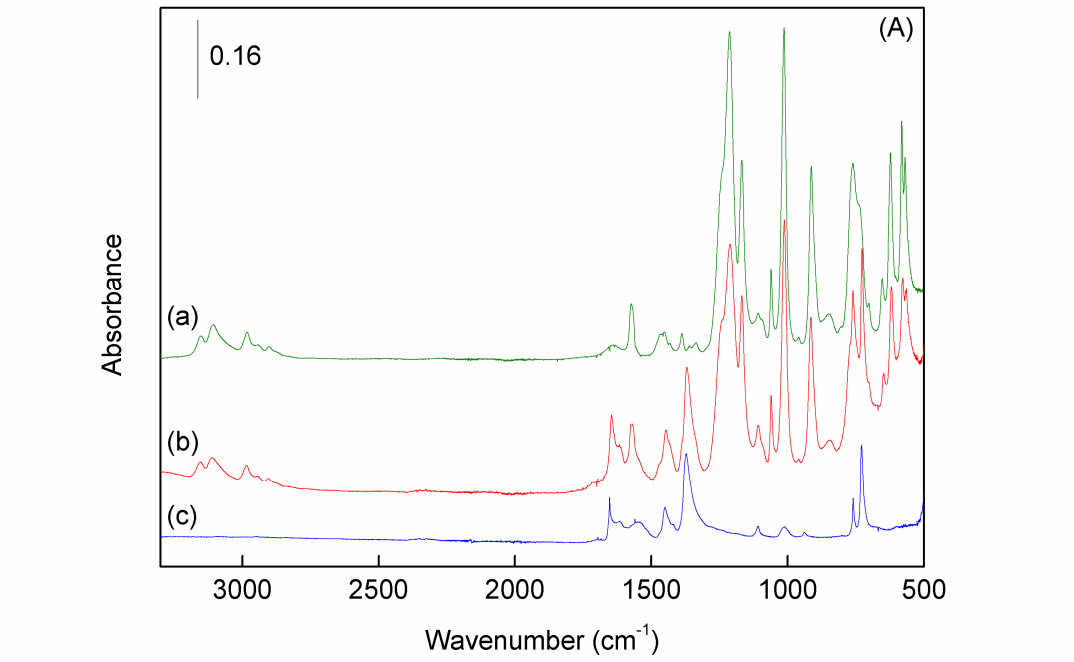

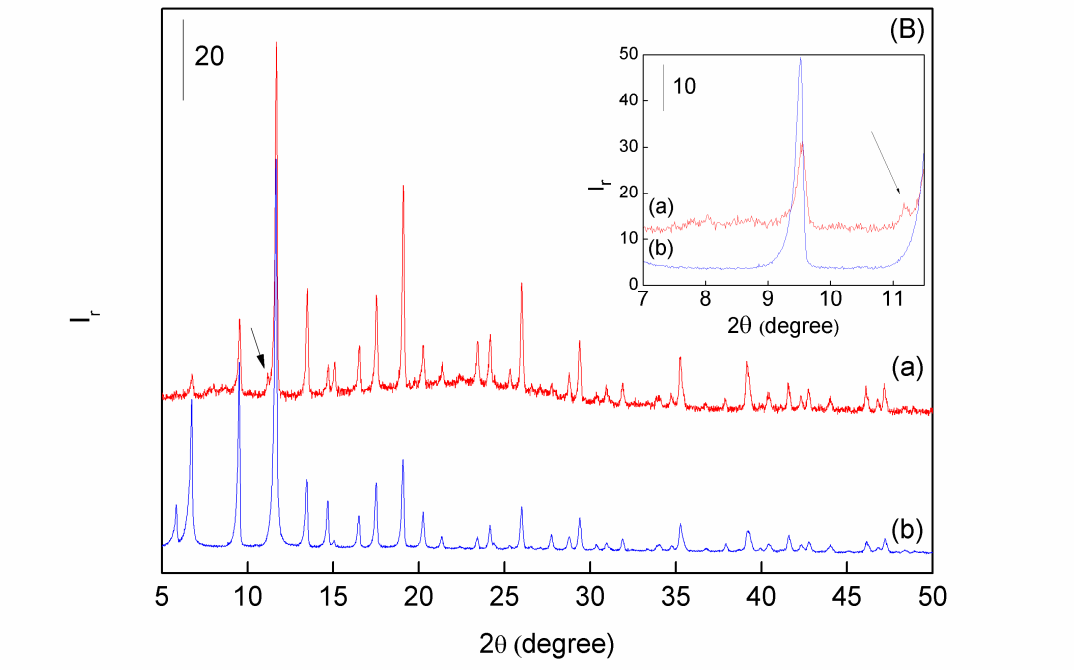

Fig. 1. A: FTIR spectra of (a) pure IL, (b) IL confined CuBTC, and (c) pristine CuBTC. B: PXRD patterns of (a) IL confined in CuBTC, and (b) pristine CuBTC.

Fig. 1B displays the PXRD patterns of the pure MOF and the sample with the IL inside. The PXRD of the EMIM-ETS/CuBTC composite shows no significant change in the bulk structure of CuBTC other than changes in the intensity of some reflections and the disappearance of the peak at 5.8º 2θ. These small changes are related to the degree of hydration.[43] Furthermore, the appearance of the weak peak at 11.1° 2θ (corresponding to the 311 plane) upon confinement of the IL is possibly due to a change in the coordination of accessible or open Cu sites by adsorption of bulkier and polar IL molecules in the pores of CuBTC. The presence of the IL in the pores reduces the adsorption of water molecules at the open Cu sites and forces the water molecules into the smaller pores.[34] Therefore, a lower number of water molecules is available for the coordination of the Cu atoms and hence the appearance of a peak at 11.1° 2θ.

Confinement of acetone, methanol and isopropanol

The analysis of the nature of organic solvents confined in the MOF has basically two aims: firstly, to gain insight into the molecular interactions between CuBTC and the three common organic solvents and, secondly, to investigate the stability of the MOF when exposed to the solvents. For the FTIR measurements, a small amount of MOF was placed on the diamond crystal of the ATR unit and then a drop of the solvent was added, similar to the recently proposed solvent infrared spectroscopy method.[44] As the solvents considered are highly volatile, it was difficult to state the exact molecular ratio. However, an excess of solvent can be assumed. Figure 2 shows the fingerprint region of the FTIR spectra of the pure solvents and the

MOF/solvent samples. For completeness, the full spectral range is provided in Fig. S1 of the supplementary material.

Acetone. The FTIR spectrum of the acetone/MOF system shows the characteristic bands of acetone at 1713, 1220 and 530 cm^{-1} (Fig. 2f), which can be assigned to C=O stretching, C-C-C stretching, and C=O out-of-plane bending modes of acetone, respectively. All other bands of acetone (1751,1440, 1420, 1358, 1092, 901 and 784 cm^{-1}) overlap with the bands of the CuBTC. Therefore, any frequency changes related either to CuBTC or to acetone are difficult to determine unambiguously. Interestingly, no perturbation of the acetone bands at 1713, 1220, and 530 $cm^{-1}$was observed. However, four new features appear at 1700, 1704, 1235, and 543 cm^{-1} upon the confinement of acetone in CuBTC. The band at 1700 and 1235 cm^{-1} can be attributed to carboxylic acid (combination band of C=O and C-OH). The band at 543 cm^{-1} corresponds to an in-plane bending mode of coordinated molecular water (indicated by arrows in Fig. 2f). The appearance of carboxylic acid bands[45] in the CuBTC + acetone system provides a clear molecular level insight about the interactions between the carboxylate groups of CuBTC and acetone. As a result of these interactions, a certain fraction of the carboxylate groups of CuBTC are converted into carboxylic acid. This means that CuBTC promotes hydrolysis in the presence of acetone. The water, which is necessary for this reaction, originates from the CuBTC sample itself. CuBTC is highly hygroscopic and usually contains small amounts of adsorbed water molecules, even after extensive drying. From the observed extent of hydrolysis, it can be concluded that acetone is not a suitable solvent for post synthetic modifications of CuBTC, at least not if the MOF contains small amounts of adsorbed water.

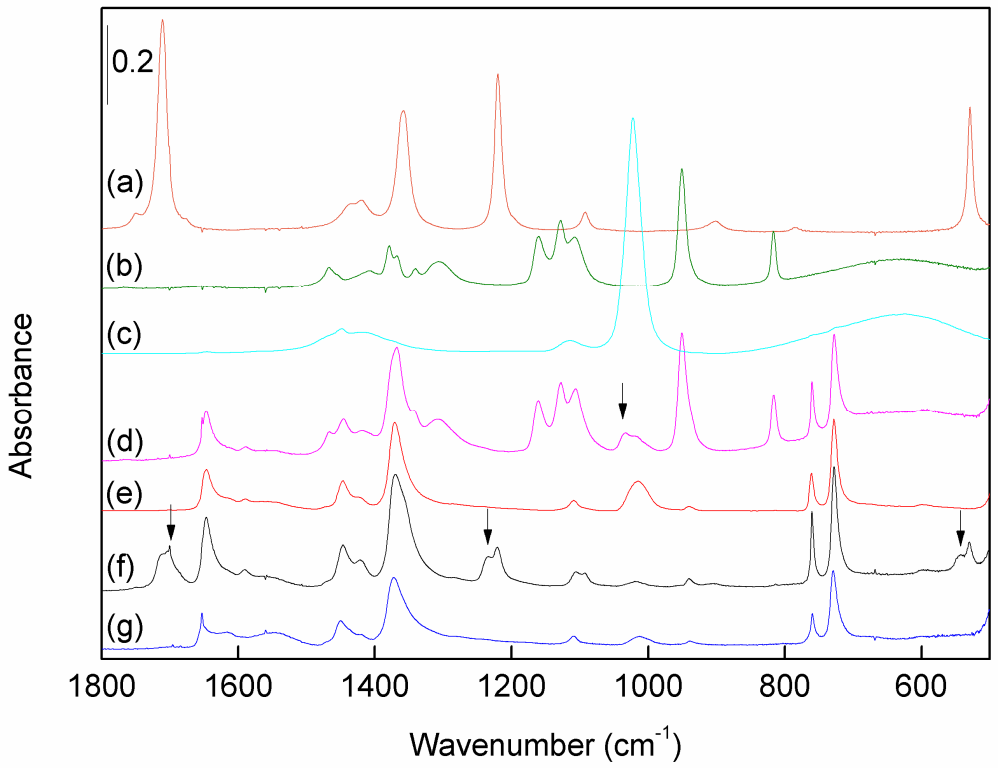

Fig. 2 FTIR spectra of the pure solvents: (a) acetone, (b) isopropanol, (c) methanol,and confined systems (d) CuBTC with isopropanol, (e) CuBTC with methanol, (f) CuBTC with acetone,(g) pristine CuBTC.

Isopropanol. The main infrared bands in the spectrum of isopropanol are observed at 817 cm^{-1} (C-C stretch), 951 cm^{-1} (CH_3 rock), 1128 and 1161 cm^{-1} (CH_3 rock & C-C stretch), 1341 cm^{-1} (CH wag), 1368 and 1379 cm^{-1} (CH_3 symmetric deformation), 1107, 1306, and 1407 cm^{-1} (in-plane deformation of H atom in COH group in alcohol), 1467 cm^{-1} (CH_3 antisymmetric deformation), 2882, 2933, and 2971 cm^{-1} (CH stretch), and 3500-3000 cm^{-1} (OH stretch). The confinement of isopropanol in CuBTC produces no significant changes in the vibrational frequencies of either the CuBTC or the isopropanol bands. However, a new band is observed at 1035 cm^{-1}, as indicated by the arrow in Fig. 2d. This new band is likely related to the C−O

vibration as a result of the interaction between isopropanol and the carboxylate groups of CuBTC.

Methanol. The spectra show that all the infrared bands related to CuBTC and methanol are found at the same frequencies (Fig. 2e) as in the spectra of the individual components. Hence, the confinement of methanol in CuBTC has no impact on the chemical nature of either compound. Additionally, no evidence of transformation of the carboxylate groups to their analogous protonated acid is observed. This shows that methanol, unlike the acetone, does not promote hydrolysis of CuBTC.

Comparison. A comparison of the results described above shows that the interactions between isopropanol with CuBTC are significantly less pronounced than those between acetone and CuBTC. In the methanol/CuBTC system no changes to the vibrational spectrum were found. Therefore, it can be concluded that methanol has the least impact on the structure of CuBTC. Hence, it is well suited as a solvent for post synthetic modifications of CuBTC, e.g. in the impregnation or removal of other substances such as an IL.

Stability of CuBTC in acetone, isopropanol, and methanol

The stability of CuBTC in the presence of water has been studied many times and it was shown that hydrolysis reactions can lead to destruction of the MOF structure[43,46,47]. Therefore, water is generally unsuitable, for example, as an extraction medium to remove confined molecules from the porous matrix of the MOF. The suitability of acetone, isopropanol, and methanol for this purpose was evaluated by investigating the stability of the MOF in the presence of the individual solvents. In the first step, the stability of CuBTC was studied by immersing the MOF in acetone,

isopropanol, or methanol for 5 h. For comparison, the same procedure was applied to water. The immersed CuBTC samples were then filtered, dried in an oven at 70 and 150 ºC for 24 h at each temperature, and then analyzed. The FTIR spectra recorded after the drying procedure are shown in Fig. S2 in the supplementary material. Heating at 70 ºC for 24 h is insufficient to completely remove the solvents from CuBTC as the spectra show signs of residual solvents (spectra c and e of Fig. S2). In contrast, FTIR spectra after drying at 150 °C show virtually no traces of the solvents (spectra a, d, and g of Fig. S2). In case of acetone when heated at 70 ºC for 24 h, the spectrum shows a weak peak at 1704 cm^{-1}. The intensity of this peak due to residual acetone was decreased significantly by heating at 150 ºC (spectrum d of Fig. S2). The stability of the structure for the washed samples was further investigated by PXRD and compared with pristine CuBTC (Fig. 3). The PXRD patterns of CuBTC washed with solvents are very similar to the pattern of pristine CuBTC. This indicates the intactness or structural stability of the MOF after the washing procedure.

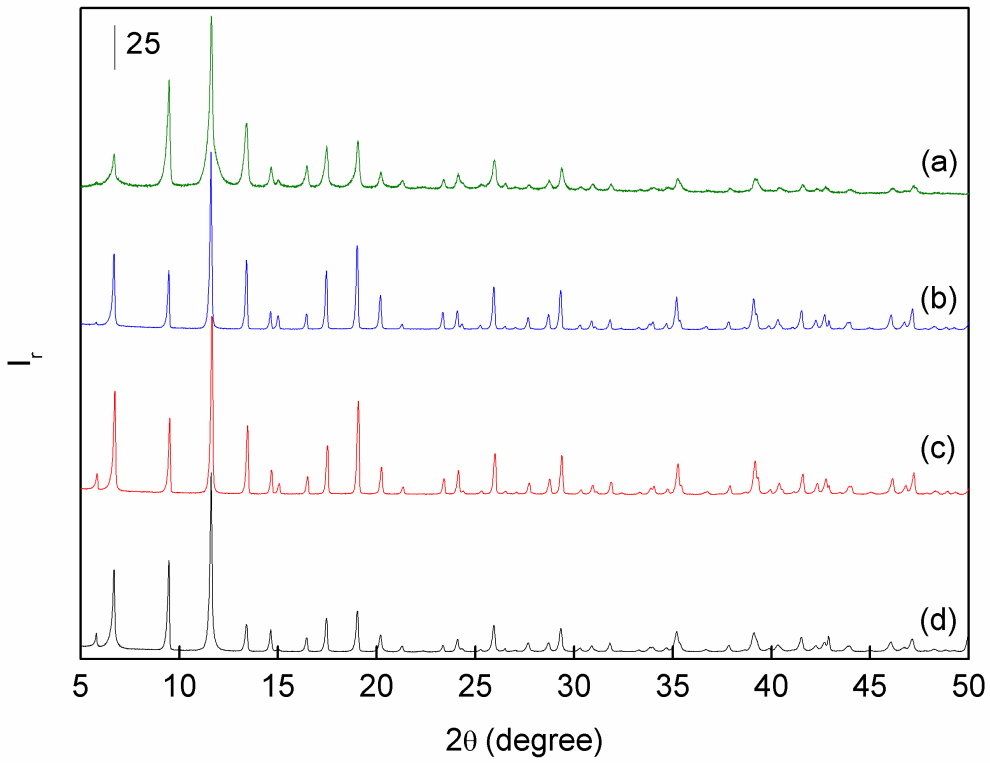

Fig. 3. PXRD of CuBTC washed with solvents and heated at 70 °C for 24 h (a) CuBTC washed with methanol (b) CuBTC washed with isopropanol (c) CuBTC washed with acetone (d) pristine CuBTC.

These findings are supported by observations using SEM (Fig. 4) which show that the morphology of the particles remain virtually identical. The SEM micrographs of the washed samples show the crystals as possessing very smooth surfaces. This is a clear indication that there is no degradation of the external surface when exposed to isopropanol or methanol. Small changes in terms of crumples at the external surface of CuBTC crystals are observed in the case of acetone (Fig. 4b). This supports the findings based on FTIR evidence for the promotion of the hydrolysis reactions of the MOF in the presence of acetone.

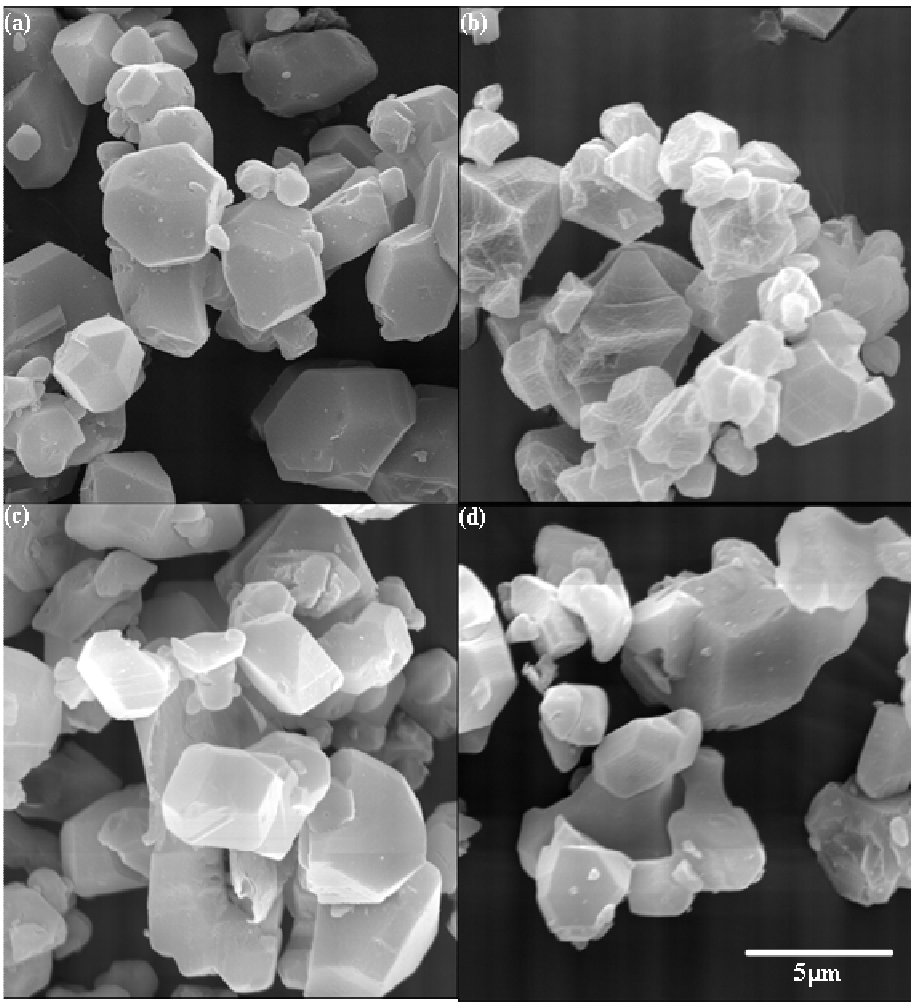

Fig. 4.SEM micrographs of CuBTC (a) in pristine state, (b) after washing with acetone, (c) after washing with isopropanol, and (d) after washing with methanol

The N_2 adsorption isotherms of CuBTC before and after washing show similar microporous nature (Fig.5). The BET surface area and the pore volumes (t-plot) of CuBTC washed with acetone, isopropanol, and methanol are: 2006 m^2/g and 0.61cm^3/g, 1984 m^2/g and 0.66 cm^3/g, and 1992 m^2/g and 0.62cm^3/g, respectively. These values are very close to the corresponding data for pristine CuBTC (2050 m^2/g and 0.64 cm^3/g) pretreated at 150°C. Therefore, from a stability point of view, it can conclude that isopropanol and methanol are suitable extraction media as they can be completely removed from the MOF without causing changes to the molecular structure of CuBTC. Acetone is in principle suitable as well, in that the physisorption

characteristics are returned following exposure and solvent removal. However, the potential to promote hydrolysis in hydrated MOF needs to be kept in mind. The concept of using these solvents for extraction purposes have been investigated in the context of removal of IL from impregnated CuBTC and will be discussed in following section.

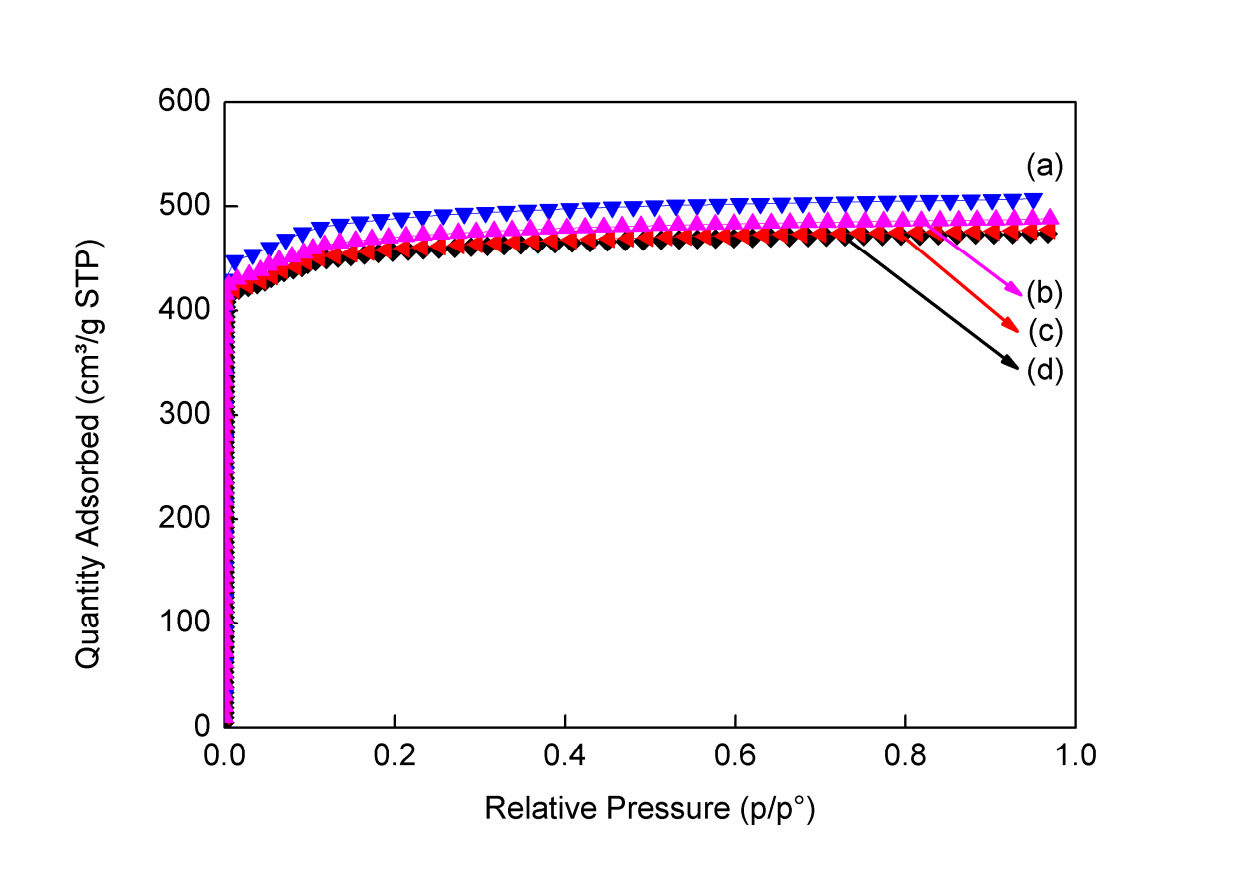

Fig. 5. Nitrogen isotherms at -196 °C CuBTC exposed to different solvents: (a) isopropanol, (b) methanol, (c) acetone, and (d) pristine CuBTC.

Removal of confined IL from CuBTC using organic solvents

The three organic solvents as well as water were tested for their efficiency in the extraction of the IL EMIM-ETS from CuBTC. Water has been employed in similar applications frequently[28,29,48] and is therefore used as a reference case here. The impact of water on the

structural stability of CuBTC was analyzed in a previous study.[43] It was found that the Cu-based MOF was structurally stable in the presence of small amounts of water during short-term exposure. However, exposure of CuBTC to liquid water or ambient moisture for longer periods of time resulted in irreversible changes due to hydrolysis reactions. The removal or washing of IL from impregnated CuBTC with water will be discussed in more detail in the next section.

The consequences of removal of the IL from the pores of CuBTC was investigated by FTIR spectroscopy with Fig. 6 showing spectra after the washing procedure employing different solvents. For the washing, an IL impregnated CuBTC sample (20 mole % CuBTC with IL) was emerged in 10 ml of methanol, acetone, or isopropanol for 5 h and then filtered and dried at 70 °C for 24 h. The CH stretching region from 3200 to 2700 cm^{-1} (inset in Fig. 6) is selected to assess the presence of the IL in the washed CuBTC or in the IL extracted CuBTC. Acetone was not capable of completely removing the IL from the CuBTC in the first wash as revealed by the characteristic IL peaks at 3151 and 3106 cm^{-1} in the spectrum of the washed sample (spectrum c in inset of Fig. 6. Spectrum b in Fig. 6 indicates that isopropanol is more effective than acetone although a very small amount of IL was retained. This remaining amount of IL was removed by repeating the washing cycle. Spectrum d in Fig. 6 suggests that methanol is a very effective solvent for removing the IL completely from the impregnated CuBTC following the very first washing cycle.

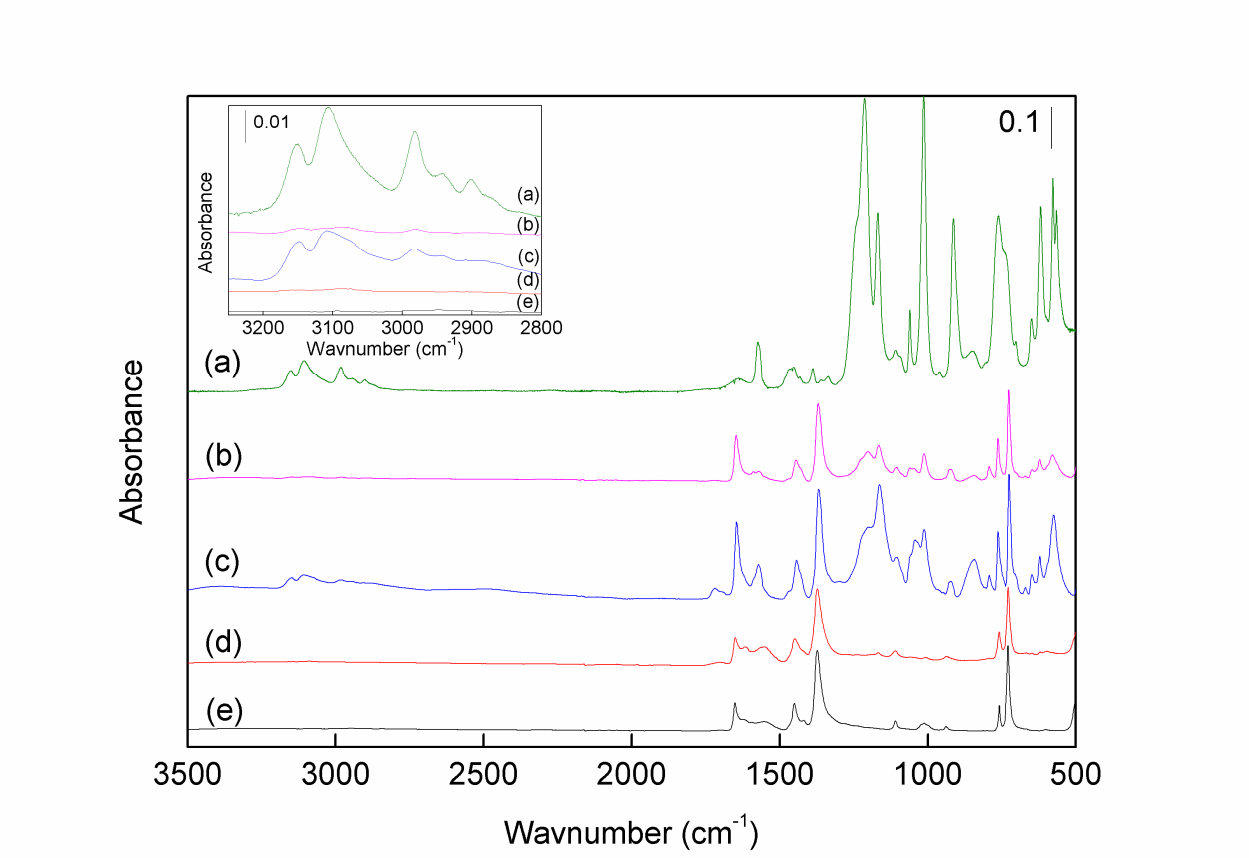

Fig. 6 FTIR spectra of (a) pure IL and CuBTC after IL extraction with the solvent (b) isopropanol, (c) acetone, (d) methanol, and (e) pristine CuBTC.

The data discussed in the preceding sections indicated that the organic solvents (except acetone) had no or limited impact on the crystal structure of CuBTC. However, a possibility exists that the combination of solvent and IL inside the pores of MOF may lead to structural alterations. In binary mixtures of the IL and solvents[42,49] the ion-pairs of the IL can dissociate, in particular in the presence of large amounts of solvent. The dissociated ion-pairs may have a different impact on the structural stability of CuBTC. PXRD measurements were performed on the IL extracted CuBTC samples and the pattern after extraction with methanol is shown in Fig. S3. The data do not indicate any changes in the bulk structure of CuBTC as all reflections of pristine CuBTC can be observed in the sample from which the IL was removed with the help of methanol. However,

there are some minor changes in the intensity of some reflections which could be related to the degree of hydration.[50] The sample after IL extraction with methanol was further investigated by SEM (Fig. 7) in order to determine if any changes in the morphology and the external surface of the CuBTC crystals had taken place. Sharp well-defined edges and smooth outer surfaces of the crystals exhibiting octahedral shape are observed and the overall appearance is very similar to the surface morphology of pristine CuBTC crystals (Fig. 4a).

Overall, experiments conducted with the IL impregnated CuBTC after washing with methanol, acetone, and isopropanol suggest that methanol is best suited for extracting the IL from the MOF. It does not affect the crystalline structure, interacting sites, and surface morphology of CuBTC suggesting that it does not promote hydrolysis reactions. The greater efficiency of methanol to remove the IL compared to acetone and isopropanol is attributed to its higher dielectric constant.

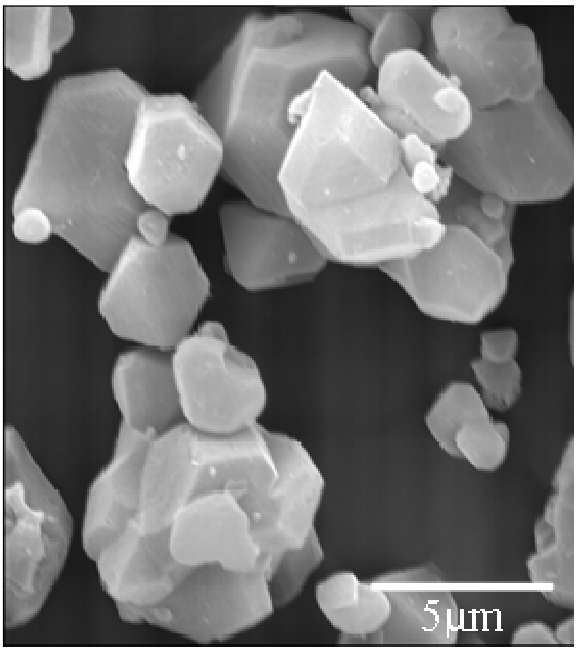

Fig. 7 SEM micrograph of CuBTC after removal of IL with methanol from impregnated CuBTC.

Stability ofIL impregnated and pristine CuBTC under molecular water

Structural analysis. Removal of the IL from the impregnated CuBTC was also attempted with water. The FTIR spectrum of the IL impregnated CuBTC sample after washing with water is shown in Fig. 8. On the one hand, it can be noted that no features characteristic of the IL can be found in the spectrum after the washing procedure, indicating that water removes the IL effectively. On the other hand, comparison with the spectrum of pristine CuBTC shows appearance of many new bands particularly free carboxylic acid, C-C stretching related to BTC ring and Cu-O stretching, suggesting the transformation or complete disruption of the CuBTC structure. Similar changes in the FTIR spectrum were not found when CuBTC was exposed to water for a short time periods.[43]

The FTIR spectrum of the resulting material was investigated to gain some molecular level insights. The vibrational frequencies of the pure IL,[40] the pure CuBTC,[41] the IL extracted CuBTC, and the washed CuBTC are summarized in Table 1 together with tentative assignments. Additional bands appear at similar wavenumbers for the IL extracted sample as for the washed sample, which had not been exposed to the IL. This suggests a similar product material after the exposure to water irrespective of the CuBTC history. Furthermore, the IL does not play an important role in the degradation or transformation of CuBTC in the presence of water. The appearance of new features corresponding to free carboxylic acid (1704 cm^{-1}) indicates the degradation of the carboxylate group of the MOF linker molecules. Changes in the C-C stretching vibration of the BTC ring and of the C-H out-of-plane bending of the ring indicate modifications to the surrounding molecular environment. Changes in the Cu-O stretching mode are also observed (722, 692 and 631 cm^{-1}). These findings support the hypothesis that disruption

of CuBTC in water leads to formation of a new material with a different molecular structure compared to pristine CuBTC.

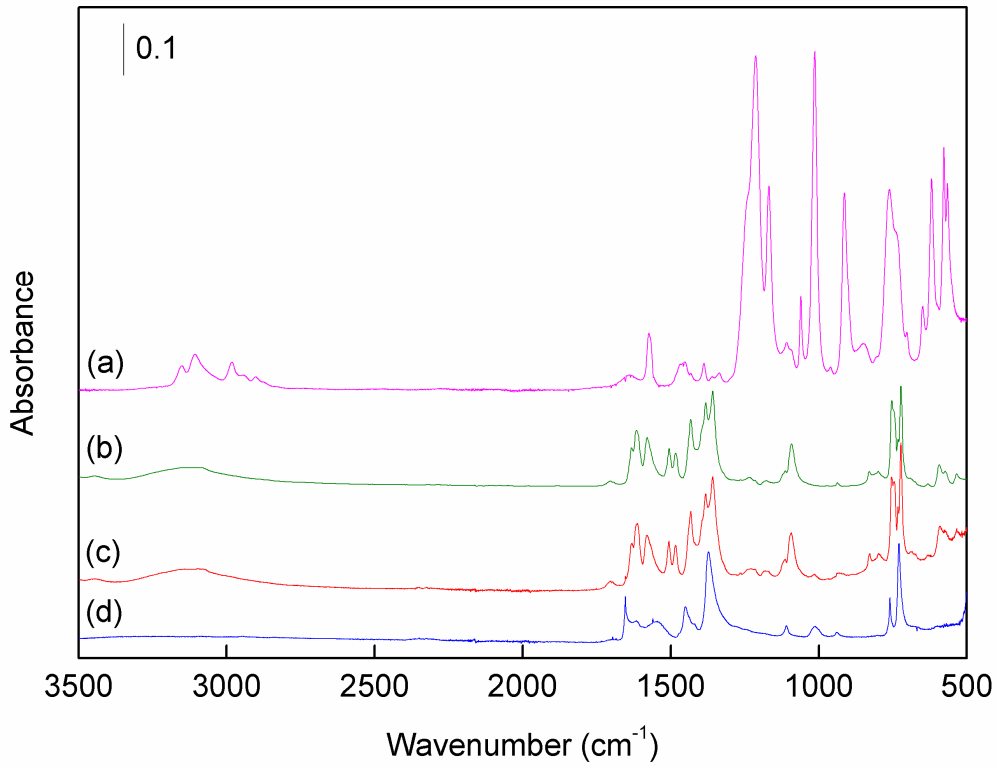

Fig. 8. FTIR spectra of (a) pure IL, (b) CuBTC washed with water and dried at 70°C for 24 h, (c) IL impregnated CuBTC after washing with water and dried at 70°C for 24 h, and (d) pristine CuBTC.

In order to gain information about the structural changes in the sample, PXRD measurements were performed. The data (Fig. 9) clearly show that the crystalline structure of the MOF is severely changed when the IL is removed by water. Note that the PXRD patterns of the pristine CuBTC washed with water and the IL extracted CuBTC look very similar. This means that the disruption of the crystal structure of CuBTC is due to the impact of water and that the IL does not play a role. However, there are some differences in the PXRD patterns. These differences can be attributed to the amount of water and the number of washing cycles. It is also noteworthy that

the washing and drying conditions have a certain impact on the resulting structure of the material (Fig. S4). The disappearance of many reflections indicates permanent changes in the phases of the washed CuBTC at elevated temperature. Generally, these alterations to the pattern can be attributed to a complete degradation of CuBTC. However, the role of water in degrading the structure of CuBTC through hydrolysis is complex and depends on various factors such as the duration of exposure and the amount of water involved.[43]

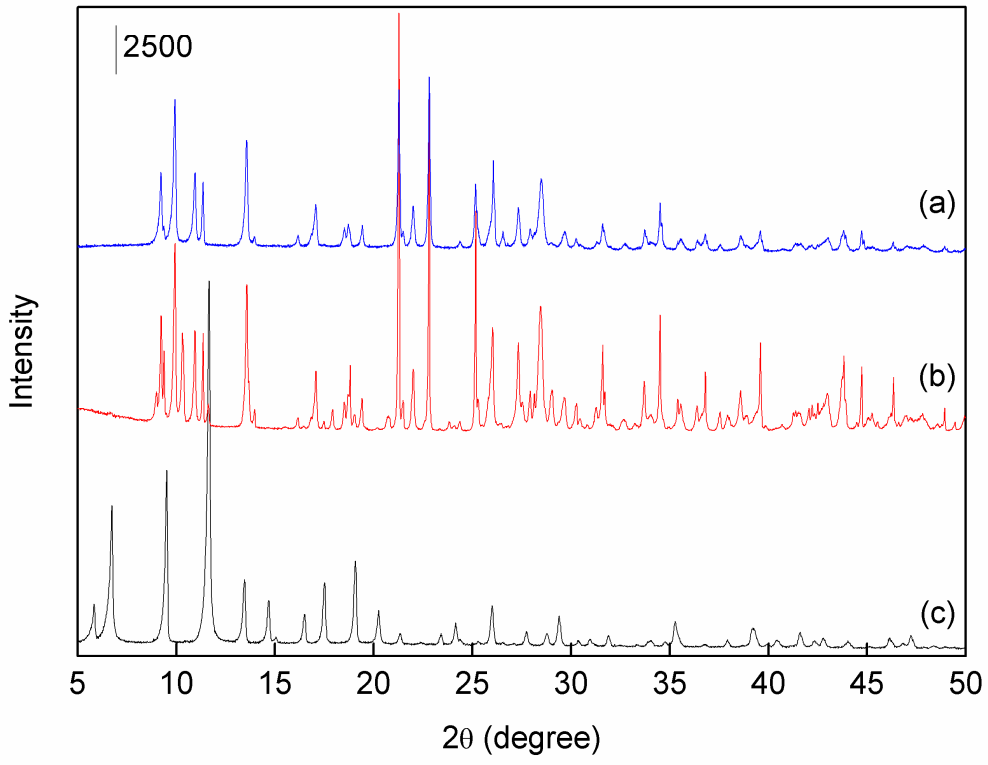

Fig. 9. PXRD patterns of washed and CuBTC dried at 70 °C for 24 h. (a) CuBTC washed with water, (b) IL impregnated CuBTC washed twice with water, and (c) pristine CuBTC.

To shed light on the nature of the resulting powder, an attempt was made to unravel the degradation mechanism and to characterize (and possibly identify) the material. During

treatment, that sample was exposed to a large amount of water. Consequently, a clustering of water molecules around the Cu atoms may enhance the hydrolysis reaction. This leads to a fast hydrolysis reaction during which the metal ligand bonds break and unknown compounds form. Possible product compounds include CuO, Cu_2O, $Cu(OH)_2$, Cu_2SO_4, $CuSO_4.5H_2O$, $Cu_2(CH_3CO_2)_4.2H_2O$, benzene-1,3,5-tri carboxylic acid or trimesic acid (BTC) with and without water, and copper (II) acetate monohydrate. Therefore, single crystal XRD patterns of all these possible compounds are plotted together with the PXRD pattern of the washed CuBTC sample (Fig. S6 of the supplementary material). Comparison shows that the IL extracted or water washed CuBTC does not exist as a single phase. Moreover, the water treated sample contains mixed phases of pristine CuBTC, trimesic acid (BTC) with and without water etc. Therefore, it is very difficult to propose or hypothesized the molecular level mechanism for disruption of crystal structure of CuBTC in water. Unfortunately, all attempts to further resolve the structural modifications from the PXRD pattern of the treated samples were unsuccessful due to the significant levels of change that had occurred. This could be due to the presence of unknown phases in the powder samples or because of the presence of an entirely different crystal structure. A more comprehensive crystallographic analysis is necessary to answer these open questions, but this is beyond the scope of the present work.

Material properties. The porous nature of the CuBTC after IL extraction was further investigated by N_2 adsorption measurements. After washing with water, the resulting microcrystalline material shows non-porous behavior (Fig. S5 in the supplementary material) and a substantially reduced surface area (less than 7 m^2/g) compared to pristine CuBTC. The BET surface area of pristine CuBTC after exposure to water for 5 h exhibits a similar surface area (19 and 11m^2/g degassed at 70 and 150 °C, respectively).

Electron microscopy (SEM and TEM) was performed on the samples to ascertain further information about the surface morphology, the shape and the size of the washed CuBTC crystals. The external surfaces and morphologies of washed CuBTC and IL extracted CuBTC crystals are very similar (Fig.10a, b). The SEM micrographs of the washed CuBTC samples reveal agglomerated flaky micro-rods, which are completely different from the well-defined and clean external surfaces of pointed hexagonal morphologies of the pristine CuBTC (inset of micrograph b of Fig. 10). The TEM images of the washed samples displayed in Fig. 10 c and d show the presence of non-uniform micro rods along with very few distorted hexagonal crystals (indicated by the arrow in image d of Fig. 10) whose external surface is not clean compared to pristine CuBTC (inset of image c of Fig. 10). TEM images recorded at different locations of the sample are shown in Fig. S7 of the supplementary material. These TEM images indicate a clear transformation of crystal structure into more than one phase (new phases with small amount of bulk/amorphous phase). This finding is in line with the conclusions from the PXRD data (Fig. 9). The presence of more than one unknown phase and crystal structure confirms the above assessment as to why the crystal structure of the water degraded CuBTC could be not unambiguously identified. So far, it is only clear that the IL impregnated or pristine CuBTC crystal structure collapses and is transformed into an unknown crystalline structure after washing with water.

The general conclusions obtained in this study in terms of solvent extraction and structural responses have wider applicability beyond the $Cu_3(BTC)_2$ and 1-ethyl-3-methylimidazolium ethyl sulfate employed here. However, solvent compatibility for example may be highly specific to the MOF/IL pair selected and thus a full analogous series of experiments to those conducted here would be required before drawing conclusions. For

instance, the extent of recovery of [NTf2]-based ionic liquids using water would be limited due to the low solubility in this solvent.

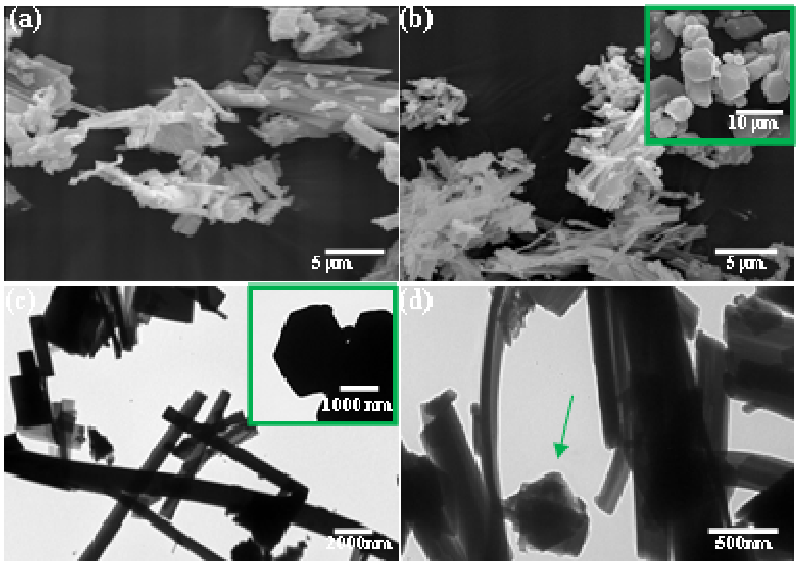

Fig. 10. SEM micrograph of (a) CuBTC washed with water and of (b) IL extracted CuBTC using water. TEM images of (c) CuBTC washed with water and (d) IL extracted CuBTC using water. Inset in panels (b) and (c) show SEM/TEM micrograph/image of pristine CuBTC respectively.

Table 1. Experimental FTIR frequencies (cm^{-1}) of pure and confined system before and after washing with water

Pure system		Confined system	Systems washed with water		Assignments*
EMIM-ETS	CuBTC	EMIM-ETS + CuBTC (20 mole%)	IL extracted CuBTC (20 mole %)	Washed CuBTC	

-	-	-	3551	3551	OH stretch of uncoordinated water
-	-	-	3499	3498	OH stretch of uncoordinated water
-	-	-	3447	3446	Molecular water
3151	-	3154	-	-	$C_{4/5}$-H stretch
3106	-	3111	-	-	C_2-H stretch
-	-	2984	-	-	C_2-H stretch
2982	-	-	-	-	Symm H_{13}-C_6-H_{14} stretch
2941, 2901	-	2942, 2905	-	-	Symm H_{29}-C_{26}-H_{31} stretch
-	-	-	1701	1704	C=O stretch of carboxylic acid
-	1652	-	1652	-	Asymmstretch (COO) (MOF)
-	-	-	1632	1632	Bending mode of water
-	1616,1547	-	1614,-	1616,-	Bending mode of adsorbed molecular water
-	-	-	1580	1580	C–C stretch (in–ring)
1571	-	1572	-	-	N_3-C_4-H_{10} rock
-	-	-	1506	1506	C–C stretch (in–ring)
-	-	-	1484	1483	C–C stretch (in–ring)
-	1450	1447	-	-	Asymm stretch (COO) (MOF)
1431	-	-	-	-	H_{12}-C_6-H_{13} rock
-	-	-	1432	1432	C–C stretch (in–ring)
-	1419	-	-	-	Symm stretch (COO) (MOF)
-	-	-	1395	1393	C–C stretch (in–ring)
1387	-	-	-	-	H_{15}-C_7-H_{16}, H_{18}-C_8-H_{19} rock
-	-	-	1382	1382	C–C stretch (in–ring)
-	1374	1369	-	-	Symm stretch (COO) (MOF)
-	-	-	1358	1358	C-O stretch
1335	-	1335	-	-	N_1-C_7-H_{16} rock

-	-	-	1264	1264	C-O stretch
1243	-	1243			N_1-C_2-H_9 rock + S_{20}-O_{23}stretch
-	-	-	1230	1234	C-OH stretch of carboxylic acid
1213	-	1213	-	-	S_{20}-O_{23} stretch
-	-	-	1215	1214	C-O stretch
-	1187	-	1187	1181	-
1169	-	1166	-	-	N_1-C_2-H_9 + O_{21}-S_{20}-O_{22}asym stretch
1108	-	1108	-		H_{29}-C_{26}-H_{30} twist
-	1112	-	1113	1113	C-H in plane bending ring (MOF)
1091	-	1089	-	-	H_{13}-C_6-H_{14} twist
-	-	-	1093	1092	-
1060	-	1060	-	-	O_{24}-C_{25} stretch
1013	-	1013	-		C_2-N_1-C_5 stretch
-	1013	-	1013	-	C-H stretch (MOF)
-	939	-	930	938	OH bending (MOF)
913	-	915	-	-	O_{21}-S_{20}-O_{22}symm stretch
-	-	-	828	830	C-H out of plane bending of ring (MOF)
807	-	-	-	-	N_1-C_2-H_9 wag
761,702	759	760,-	-	-	S-O stretching (IL), C-H out-of-plane bending of ring (MOF)
-	-	-	798	799	C-H out of plane bending of ring
-	-	-	755	753	C-H out of plane bending of ring
-	-	-	745	746	C-H out of plane bending of ring
-	-	-	733	733	C-H out of plane bending of ring
734	729	727	-	-	S_{20}-O_{24} stretch (IL),C-H out of plane bending of ring (MOF)
-	-	-	722	722	C-H out of plane bending of ring + Cu-O stretch
-	-	-	687	692	,,
648	-	648	-	-	C-N bonding oscillation

-		-	-	631	Cu-O stretch
618	-	620	-	-	N_1-C_7 stretch
-	-	-	590	593	C-H out of plane bending of ring + Cu-O stretch
577	-	579	-	-	O_{21}-S_{20}-O_{22} wag
-	-	-	-	573	In plane bending of adsorbed molecular water
565	-	563	-	-	-

* The assignments of the IL are based on the optimized structure of the IL reported in the literature.[40]

Conclusions

The removal of an imidazolium based IL from the pores of CuBTC MOF was investigated using FTIR, PXRD, N_2-adsorption, and electron microscopy. Acetone, isopropanol, methanol, and water were employed as extraction media. Acetone and isopropanol were unable to completely remove the confined IL, whereas water shows good capability, but it a substantially negative impact on porous and crystal structure of the MOF. Methanol was identified as the most suitable solvent to remove the confined IL from CuBTC. It effectively removed the IL without affecting the MOF structure.

In addition, the confinement of acetone, isopropanol, and methanol in CuBTC was studied in order to distinguish between the effects of the treatments by solvent alone and its combination with the IL. The data revealed weak interactions between the carboxylate groups of CuBTC with acetone and isopropanol through hydrogen bonding. However, no such interactions were found in case of methanol and CuBTC. CuBTC is stable in all the organic solvents tested, but acetone promoted the hydrolysis in the slightly hydrated MOF sample. On the other hand, exposing the MOF to water, leads to structural changes. This instability of CuBTC in water is related to the

breaking of metal ligand bonds as a result of hydrolysis reactions. The hydrolysis reaction depends on parameters such as the amount of water, the duration of exposure, and the drying temperature. The IL did not play a role in the degradation mechanism. Interestingly, the material obtained as a result of the degradation still retained crystalline structure as revealed by its PXRD pattern, but does no longer retain porosity. Analysis showed that it consists of more than one phase. The degraded samples show similar morphology. SEM and TEM revealed non-uniform, agglomerated, flaky micro-rods.

This study provided valuable information about the impact of four common solvents and an imidazolium-based IL on the intrinsic chemical and structural characteristics of CuBTC MOF. The objective was to identify suitable media for post synthetic modification of MOFs. Additionally, MOFs show potential to serve as robust porous matrices that can be used several times after removal of the confined substance. Results here indicate that extraction with organic solvents is a promising route for recycling of CuBTC with no detectable loss of porosity orcrystal structure.

Supplementary information

FTIR spectra of confined solvents in CuBTC, FTIR spectra of washed CuBTC with solvents, PXRD of IL extracted CuBTC with methanol, temperature dependent PXRD of CuBTC after washing with water, Nitrogen adsorption isotherms of CuBTC and IL extracted CuBTC, comparison of XRD pattern of $Cu_2(CH_3CO_2)_4.2H_2O$, Cu_2SO_4, $CuSO_4.5H_2O$,CuO, $Cu(OH)_2$, Cu_2O, 1,3,5-benzene try carboxylic acid with two water molecules ($C_6H_3(CO_2H)_3.2H_2O$), 1,3,5-benzene try carboxylic acid ($C_6H_3(CO_2H)_3$, with activated CuBTC and IL impregnated CuBTC after washing with water.

Acknowledgements

This work was supported in part by NSF Grant No. CHE-1223988 and by EPSRC Grant No. EP/K00090X/1.

References

(1) Ohno, H. *Electrochemical Aspects of Ionic Liquids*, vol. 2.; Ohno, H., Ed.; John Wiley & Sons, Inc., Hoboken, New Jersey, 2011.

(2) *Electrodeposition from Ionic Liquids*; Endres, F., MacFarlane, D., Abbott, A., Eds.; WILEY-VCH Verlag GmbH & Co. KGaA Weinheim, 2008.

(3) Brennecke, J. F.; Rogers, R. D.; Seddon, K. R. *Ionic Liquids IV Not Just Solvents Anymore*; ACS SYMPOSIUM SERIES 975: American Chemical Society: Washington, DC, 2007.

(4) Singh, M. P.; Mandal, S. K.; Verma, Y. L.; Gupta, A. K.; Singh, R. K.; Chandra, S. Viscoelastic, Surface, and Volumetric Properties of Ionic Liquids [BMIM][OcSO4], [BMIM][PF6], and [EMIM][MeSO3]. *J. Chem. Eng. Data* **2014**, *59*, 2349–2359.

(5) Ohno, H. *Electrochemical Aspects of Ionic Liquid*, vol. 1.; Wiley & Sons, Inc., Hoboken, New Jersey, 2005.

(6) Cook, T. R.; Zheng, Y. R.; Stang, P. J. Metal-Organic Frameworks and Self-Assembled Supramolecular Coordination Complexes: Comparing and Contrasting the Design, Synthesis, and Functionality of Metal-Organic Materials. *Chem. Rev.* **2013**, *113*, 734–777.

(7) Jiang, J.; Yaghi, O. M. Brønsted Acidity in Metal–Organic Frameworks. *Chem. Rev.* **2015**, *115*, 6966–6997.

(8) Silva, P.; Vilela, S. M. F.; Tome, J. P. C.; Almeida Paz, F. A. Multifunctional Metal-Organic Frameworks: From Academia to Industrial Applications. *Chem. Soc. Rev.* **2015**, *44*, 6774–6803.

(9) Schneemann, A.; Bon, V.; Schwedler, I.; Senkovska, I.; Kaskel, S.; Fischer, R. A. Flexible Metal–organic Frameworks. *Chem. Soc. Rev.* **2014**, *43*, 6062–6096.

(10) Odoh, S. O.; Cramer, C. J.; Truhlar, D. G.; Gagliardi, L. Quantum-Chemical Characterization of the Properties and Reactivities of Metal–Organic Frameworks. *Chem. Rev.* **2015**, *115*, 6051–6111.

(11) Qiu, S.; Xue, M.; Zhu, G. Metal-Organic Framework Membranes: From Synthesis to Separation Application. *Chem. Soc. Rev.* **2014**, *43*, 6116–6140.

(12) Rosseinsky, M. J. Recent Developments in Metal-Organic Framework Chemistry: Design, Discovery, Permanent Porosity and Flexibility. *Microporous Mesoporous Mater.* **2004**, *73*, 15–30.

(13) Rowsell, J. L. C.; Yaghi, O. M. Metal-Organic Frameworks: A New Class of Porous Materials. *Microporous Mesoporous Mater.* **2004**, *73*, 3–14.

(14) Stock, N.; Biswas, S. Synthesis of Metal-Organic Frameworks (MOFs): Routes to Various MOF Topologies, Morphologies, and Composites. *Chem. Rev.* **2012**, 933–969.

(15) Furukawa, H.; Cordova, K. E.; O'Keeffe, M.; Yaghi, O. M. The Chemistry and Applications of Metal-Organic Frameworks. *Science* **2013**, *341*, 1230444 (1-12).

(16) Lee, J.; Farha, O. K.; Roberts, J.; Scheidt, K. A.; Nguyen, S. T.; Hupp, J. T. Metal-Organic Framework Materials as Catalysts. *Chem. Soc. Rev.* **2009**, *38*, 1450–1459.

(17) Sumida, K.; Rogow, D. L.; Mason, J. A.; McDonald, T. M.; Bloch, E. D.; Herm, Z. R.; Bae, T. H.; Long, J. R. Carbon Dioxide Capture in Metal-Organic Frameworks. *Chem. Rev.* **2012**, *112*, 724–781.

(18) Horcajada, P.; Gref, R.; Baati, T.; Allan, P. K.; Maurin, G.; Couvreur, P.; Férey, G.; Morris, R. E.; Serre, C. Metal Organic Frameworks in Biomedicine. *Chem. Rev.* **2012**, *112*, 1232–1268.

(19) Kreno, L. E.; Leong, K.; Farha, O. K.; Allendorf, M.; Duyne, R. P. Van; Hupp, J. T. Metal

À Organic Framework Materials as Chemical Sensors. *Chem. Rev.* **2011**, *112*, 1105–1125.

(20) Singh, M. P.; Singh, R. K.; Chandra, S. Ionic Liquids Confined in Porous Matrices: Physicochemical Properties and Applications. *Prog. Mater. Sci.* **2014**, *64*, 73–120.

(21) Verma, Y. L.; Singh, M. P.; Singh, R. K. Effect of Ultrasonic Irradiation on Preparation and Properties of Ionogels. *J. Nanomater.* **2012**, *2012*, 1–6.

(22) Bellayer, S.; Viau, L.; Tebby, Z.; Toupance, T.; Bideau, J. Le; Vioux, A. Immobilization of Ionic Liquids in Translucent Tin Dioxide Monoliths by Sol–gel Processing. *Dalt. Trans.* **2009**, 8, 1307–1313.

(23) Chen, S.; Kobayashi, K.; Miyata, Y.; Imazu, N.; Saito, T.; Kitaura, R.; Shinohara, H. Morphology and Melting Behavior of Ionic Liquids inside Single-Walled Carbon Nanotubes. *J. Am. Chem. Soc.* **2009**, *131*, 14850–14856.

(24) Im, J.; Cho, S. D.; Kim, M. H.; Jung, Y. M.; Kim, H. S.; Park, H. S. Anomalous Thermal Transition and Crystallization of Ionic Liquids Confined in Graphene Multilayers. *Chem. Commun.* **2012**, *48*, 2015–2017.

(25) Göbel, R.; White, R. J.; Titirici, M.-M.; Taubert, A. Carbon-Based Ionogels: Tuning the Properties of the Ionic Liquid via Carbon–ionic Liquid Interaction. *Phys. Chem. Chem. Phys.* **2012**, *14*, 5992–5997.

(26) Singh, M. P.; Verma, Y. L.; Gupta, A. K.; Singh, R. K.; Chandra, S. Changes in Dynamical Behavior of Ionic Liquid in Silica Nano-Pores. *Ionics* **2014**, *20*, 507–516.

(27) Gupta, A. K.; Vermal, Y. L.; Singh, M. P.; Singh, R. K. Role of Reduced Precursor and Solvolytic Reagent Molar Ratio on Preparation and Properties of Ionogel. *J. Solid State Chem.* **2016**, *242*, 29–37.

(28) Gupta, A. K.; Verma, Y. L.; Singh, R. K.; Chandra, S. Studies on an Ionic Liquid

Confined in Silica Nanopores: Change in T G and Evidence of Organic–Inorganic Linkage at the Pore Wall Surface. *J. Phys. Chem. C* **2014**, *118*, 1530–1539.

(29) Verma, Y. L.; Gupta, A. K.; Singh, R. K.; Chandra, S. Preparation and Characterisation of Ionic Liquid Confined Hybrid Porous Silica Derived from Ultrasonic Assisted Non-Hydrolytic Sol-Gel Process. *Microporous Mesoporous Mater.* **2014**, *195*, 143–153.

(30) Singh, M. P.; Singh, R. K.; Chandra, S. Studies on Imidazolium-Based Ionic Liquids Having a Large Anion Confined in a Nanoporous Silica Gel Matrix. *J. Phys. Chem. B* **2011**, *115*, 7505–7514.

(31) Lee, S. H.; Doan, T. T. N.; Ha, S. H.; Koo, Y. M. Using Ionic Liquids to Stabilize Lipase within Sol-Gel Derived Silica. *J. Mol. Catal. B Enzym.* **2007**, *45*, 57–61.

(32) Shi, F.; Zhang, Q.; Li, D.; Deng, Y. Silica-Gel-Confined Ionic Liquids: A New Attempt for the Development of Supported Nanoliquid Catalysis. *Chem. - A Eur. J.* **2005**, *11*, 5279–5288.

(33) Zhang, J.; Zhang, Q.; Li, X.; Liu, S.; Ma, Y.; Shi, F.; Deng, Y. Nanocomposites of Ionic Liquids Confined in Mesoporous Silica Gels: Preparation, Characterization and Performance. *Phys. Chem. Chem. Phys.* **2010**, *12*, 1971–1981.

(34) Gutiérrez-Sevillano, J. J.; Vicent-Luna, J. M.; Dubbeldam, D.; Calero, S. Molecular Mechanisms for Adsorption in Cu-BTC Metal Organic Framework. *J. Phys. Chem. C* **2013**, *117*, 11357–11366.

(35) Van Assche, T. R. C.; Duerinck, T.; Gutiérrez Sevillano, J. J.; Calero, S.; Baron, G. V.; Denayer, J. F. M. High Adsorption Capacities and Two-Step Adsorption of Polar Adsorbates on Copper-Benzene-1,3,5-Tricarboxylate Metal-Organic Framework. *J. Phys. Chem. C* **2013**, *117*, 18100–18111.

(36) Peterson, V. K.; Southon, P. D.; Halder, G. J.; Price, D. J.; Bevitt, J. J.; Kepert, C. J. Guest Adsorption in the Nanoporous Metal−Organic Framework Cu_3(1,3,5-Benzenetricarboxylate)$_2$: Combined In Situ X‑ray Diffraction and Vapor Sorption. *Chem. Mater.* **2014**, *26*, 4712–4723.

(37) Chui, S. S.-Y.; Lo, S. M.-F.; Charmant, J. P. H.; Orpen, A. G.; Williams, I. D. A Chemically Functionalizable Nanoporous Material [$Cu_3(TMA)_2(H_2O)_3]_n$. *Science* **1999**, *283*, 1148–1150.

(38) Kiefer, J.; Fries, J.; Leipertz, A. Experimental Vibrational Study of Imidazolium-Based Ionic Liquids: Raman and Infrared Spectra of 1-Ethyl-3-Methylimidazolium Bis(trifluoromethylsulfonyl)imide and 1-Ethyl-3-Methylimidazolium Ethylsulfate. *Appl. Spectrosc.* **2007**, *61*, 1306–1311.

(39) Kiefer, J.; Namboodiri, M.; Kazemi, M. M.; Materny, A. Time-Resolved Femtosecond CARS of the Ionic Liquid 1-Ethyl-3-Methylimidazolium Ethylsulfate. *J. Raman Spectrosc.* **2015**, *46*, 722–726.

(40) Dhumal, N. R.; Kim, H. J.; Kiefer, J. Electronic Structure and Normal Vibrations of the 1-Ethyl-3-Methylimidazolium Ethyl Sulfate Ion Pair. *J. Phys. Chem. A* **2011**, *115*, 3551–3558.

(41) Dhumal, N. R.; Singh, M. P.; Anderson, J. A.; Kiefer, J.; Kim, H. J. Molecular Interactions of a Cu-Based Metal Organic Framework with a Confined Imidazolium-Based Ionic Liquid: A Combined Density-Functional Theory and Experimental Vibrational Spectroscopy Study. *J . Phys. Chem. C* **2016**, *120*, 3295–3304.

(42) Kiefer, J.; Molina, M. M.; Noack, K. The Peculiar Nature of Molecular Interactions between an Imidazolium Ionic Liquid and Acetone. *ChemPhysChem* **2012**, *13*, 1213–

1220.

(43) Singh, M. P.; Dhumal, N. R.; Kim, H. J.; Kiefer, J.; Anderson, J. A. Influence of Water on the Chemistry and Structure of the Metal–Organic Framework $Cu_3(Btc)_2$. *J. Phys. Chem. C* **2016**, *120*, 17323–17333.

(44) Kiefer, J.; Grabow, J.; Kurland, H. D.; Muller, F. A. Characterization of Nanoparticles by Solvent Infrared Spectroscopy. *Anal. Chem.* **2015**, *87*, 12313–12317.

(45) DeCoste, J. B.; Peterson, G. W.; Schindler, B. J.; Killops, K. L.; Browe, M. A.; Mahle, J. J. The Effect of Water Adsorption on the Structure of the Carboxylate Containing Metal–organic Frameworks Cu-BTC, Mg-MOF-74, and UiO-66. *J. Mater. Chem. A* **2013**, *1*, 11922.

(46) Canivet, J.; Fateeva, A.; Guo, Y.; Coasne, B.; Farrusseng, D. Water Adsorption in MOFs: Fundamentals and Applications. *Chem. Soc. Rev.* **2014**, 5594–5617.

(47) Burtch, N. C.; Jasuja, H.; Walton, K. S. Water Stability and Adsorption in Metal-Organic Frameworks. *Chem. Rev.* **2014**, *114*, 10575–10612.

(48) Singh, M. P.; Singh, R. K.; Chandra, S. Thermal Stability of Ionic Liquid in Confined Geometry. *J. Phys. D. Appl. Phys.* **2010**, *43*, 92001.

(49) Noack, K.; Leipertz, A.; Kiefer, J. Molecular Interactions and Macroscopic Effects in Binary Mixtures of an Imidazolium Ionic Liquid with Water, Methanol, and Ethanol. *J. Mol. Struct.* **2012**, *1018*, 45–53.

(50) Schlichte, K.; Kratzke, T.; Kaskel, S. Improved Synthesis, Thermal Stability and Catalytic Properties of the Metal-Organic Framework Compound $Cu_3(BTC)_2$. *Microporous Mesoporous Mater.* **2004**, *73*, 81–88.

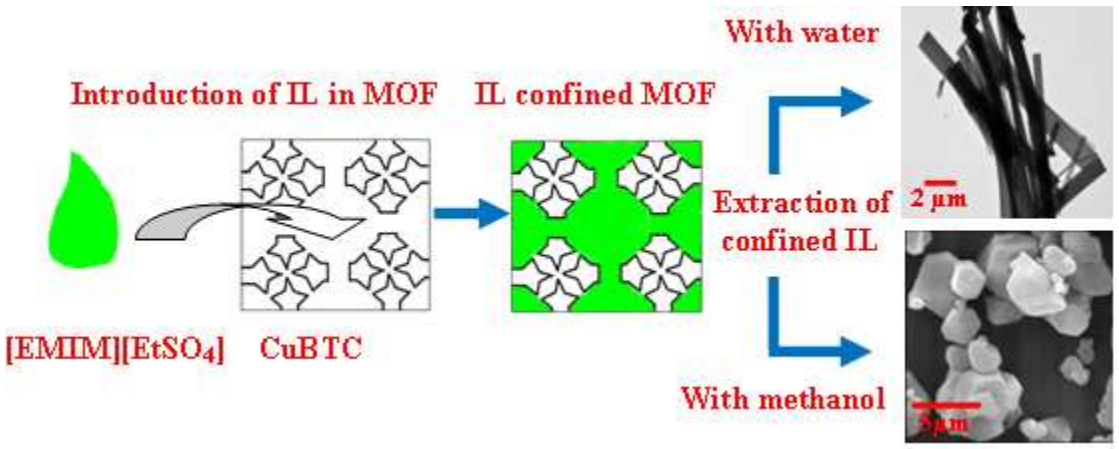
With water
Introduction of IL in MOF
IL confined MOF
Extraction of confined IL
2 µm
[EMIM][EtSO4]
CuBTC
With methanol